Hindawi
Wireless Communications and Mobile Computing
Volume 2018, Article ID 9482919, 13 pages
https://doi.org/10.1155/2018/9482919

Research Article

Low-Profile Flexible UHF RFID Tag Design for Wristbands Applications

Guan-Long Huang,[1] Chow-Yen-Desmond Sim,[2] Shu-Yao Liang,[3] Wei-Sheng Liao,[2] and Tao Yuan[4]

[1]*ATR National Key Lab. of Defense Technology, College of Information Engineering, Shenzhen University, Shenzhen 518060, China*
[2]*Department of Electrical Engineering, Feng Chia University, Taichung 40724, Taiwan*
[3]*Master's Program, College of Information and Electrical Engineering (Industrial R&D), Feng Chia University, Taichung, Taiwan*
[4]*College of Information Engineering, Shenzhen University, Shenzhen 518060, China*

Correspondence should be addressed to Chow-Yen-Desmond Sim; cysim@fcu.edu.tw

Received 14 December 2017; Revised 4 April 2018; Accepted 7 May 2018; Published 7 June 2018

Academic Editor: Mingjian Li

In this study, a low-profile ultrahigh frequency (UHF) radio-frequency identification (RFID) tag antenna designed for wristbands in healthcare applications is proposed. The radiator is based on the open-slot cavity technique that is composed of a slotted patch (double-T slots) loaded onto a flexible open cavity. The proposed slotted design can easily allow the tag's input impedance to be tuned to the complex impedance of typical UHF RFID chips. The proposed tag antenna has a size of 86 mm × 25 mm × 1.6 mm ($0.26\lambda_0 \times 0.07\lambda_0 \times 0.004\lambda_0$) at 915 MHz, and it can yield a maximum reading range of 8 m (stand alone in free-space condition), 6.6 m (when placed on the human wrist in free-space condition), and up to 3 m (when placed on the human wrist in a crowded condition).

1. Introduction

The long-term health care system has been the topic of interest discussed in recent years, and it is also now one of the most important issues in highly developed region, because the health care system in many countries has not been yet fully designed to cope with their long-term care issues. Therefore, there is a need to develop a good RFID tracking system that may require wearable devices such as a flexible RFID tag that can be used as a wristband for the patients.

In order to design an appropriate wearable RFID tag, it must be flexible and able to withstand the human body effects (or also known as on-body effects). Because of the complexity in dielectric constant within the human body (for example skin, fat, muscle, and bones), it will absorb or mitigate the electromagnetic (EM) wave emitted/received by the RFID tag. Furthermore, if the wearable RFID tag is in close proximity or directly in contact with the human body (on-body), the electrical wavelength, impedance matching, and radiation efficiency of the RFID tag will be deteriorated [1, 2]. The effects on the realized gain of an RFID tag when attached onto different body regions (arm, forearm, forehead, neck, abdomen, and stern) of a thin female volunteer were reported in [3], and they show that the stern region has the worst gain, whereas the leg region has the best gain, because of the larger content of fat tissues.

Due to the on-body effects, many different methods and techniques have been proposed to improve the performances (e.g., gain and reading range) of the RFID tag when it is at on-body condition [4, 6–12]. The easiest way to improve the reading range for on-body RFID tag monitoring application is to use an active RFID tag assisted by battery as reported in [6]; however, such method will increase the cost and thickness (profile) of the RFID tag. To achieve passive on-body RFID tag (without the assistance of battery), a planar tag antenna that is based on a suspended patch fed via a nested slot has been investigated in [7]. Even though the layout of [7]

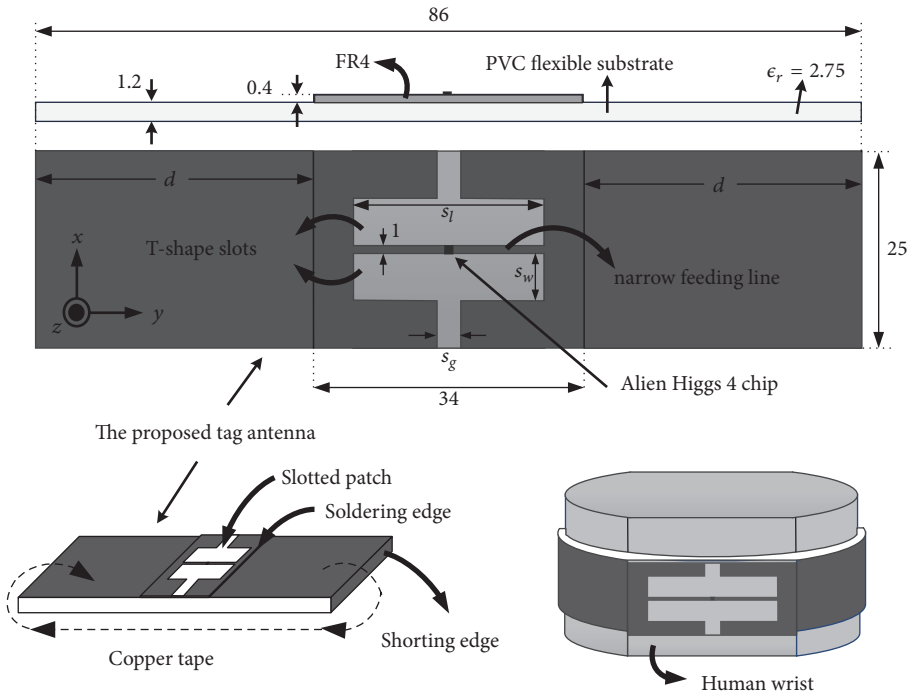

Figure 1: Geometry of the proposed tag antenna, and when it is attached to a human wrist, d = 26, S_l= 24, S_w = 6, S_g = 3. Unit: mm.

allows it to host the sensors and the slot design can be easily tuned to achieve good inductive reactance, the antenna must be electrically isolated from the skin via a 4 mm thick silicone substrate. A balanced slot-antenna concept was studied in [8] for complex environment (e.g., meat, water); however, the planar size of this tag antenna is 120 mm × 30 mm. To achieve a reading range of approximately 3.9 m (effective isotropic radiated power, EIRP 4W) when attached to the stern of a human body, a four-element PIFA array tag has been reported [9], and it has a planar size of 85.5 mm × 54 mm.

Recently, the technique of applying open-slot cavity technique for achieving on-body RFID tag designs has been reported [10–12]. To achieve compact size of 40 mm × 50 mm × 3 mm ($0.12\lambda_0 \times 0.14\lambda_0 \times 0.01\lambda_0$), the work in [10] has applied the vertical folded coupled shorted patch cavity technique, in which when attached to a human chest can achieve reading range of up to 5.1 m (EIRP 4W). As for the cavity-slot design in [11], the patches are etched on 0.4 mm thin FR4 substrate and loaded on a 1.4 mm thick foam substrate. Nevertheless, the dimensions of [11] are 116 mm ×40 mm and when attached to a human abdomen can achieve maximum reading range (R_{max}) of up to 3.5 m (EIRP 4W). As far as the author's concern, very few authors have investigated on passive RFID tag that can be applied on the wristband of a human body. In [12], two tapered structures were used to form an open-cavity structure. To achieve small size characteristics of 51.1 mm ×21.3 mm × 0.64 mm, [12] has used high dielectric constant substrate (ARLON AD1000, ε_r = 10.2), and, when attached to a human wrist, it can only yield R_{max} of up to 2.1 m (EIRP 3.23W). Nevertheless, there is no detailed reported work that has integrated a flexible wristband to a passive RFID tag that can yield R_{max} of up to 4 m with EIRP < 3W.

Therefore, in this paper, an extension of the work reported in [11] is proposed in this paper. Instead of using a rigid substrate, the slotted patch that is etched on 0.4 mm thin FR4 substrate is loaded onto a thin 1.2 mm flexible PVC (PolyVinyl Chloride) plastic substrate (ε_r = 2.75), and the open-slot cavity is formed by covering the PVC with adhesive copper tape. The advantages of this extended work as compared to the ones in [11, 12] include the following: (1) simple structure design and compact in size, (2) the wristband being flexible, and (3) ease in achieving the desired resonant frequency and impedance matching by simply tuning the slot parameters. Details of the antenna design and its corresponding simulation and measurement results (in free-space and wristband conditions) will be discussed further.

2. Antenna Structure

As aforementioned, the proposed tag antenna proposed here is an extension of the work in [11], and its geometry (including how it is attached to a human wrist) is defined in Figure 1. Here, the bottom surface (ground) of the flexible substrate is fully metalized by using the adhesive copper tape, and the two open-ends of this ground are shorted to the two rectangular copper tapes attached on the top surface (left and right sections, each has size of 26 mm × 25 mm) of the PVC. Thereafter, the two open-ends of these two copper tapes (top left and right sections) are then soldered to the two open edges of the slotted patch. By shorting the top and bottom metallic surfaces (see Figure 1), the achieved inductive reactance will compensate the tag chip's capacitive reactance.

As indicated in Figure 1, the slotted patch is formed by loading two symmetrical T-shaped slots into a 34 mm ×

Table 1: Various electrical properties of human wrist/arm phantom at 915 MHz.

	Dielectric Constant	Loss Tangent	Conductivity (S/m)
Skin (dry)	41.3	0.415	0.87
Fat	5.46	0.185	0.05
Muscle	55	0.339	0.94
Bone Cortical	12.44	0.229	0.145
Bone Cancellous	20.75	0.325	0.34
Bone Marrow	5.5	0.145	0.04

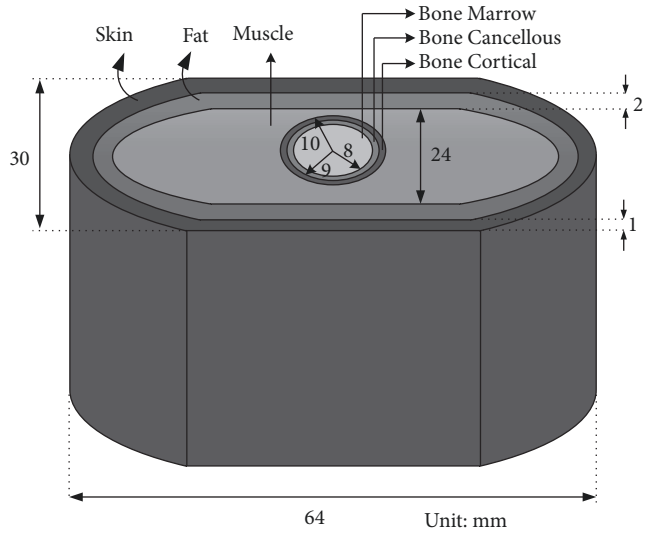

Figure 2: Various parameters (skin, fat, muscle, and bones) with reference to a human wrist/arm [4, 5] and its corresponding geometry.

25 mm rectangular patch. Each T-shaped slot is comprised of a vertical (6 mm × 3 mm) slot and a horizontal (6 mm × 24 mm) slot section. Therefore, a very narrow (1 mm) feeding line is formed between the two T-shaped slots, which is designated for connecting to the tag chip (Alien Higgs 4, SOT232 package, $Z = 8 - j142\ \Omega$). It is noteworthy that the two T-shaped slots also provide an extra degree of freedom to tune to the desired conjugate match and working frequency. The geometry of how the proposed wristband tag antenna is attached to a human wrist is also shown in Figure 1. The exact detailed structure of a human wrist/arm (skin, fat, muscle, and bones) phantom at 915 MHz, corresponding to its geometry such as substrate layers and thickness, is shown in Figure 2 [4, 5]. Its various electrical properties such as dielectric constant, loss tangent, and conductivity are also shown in Table 1. All simulations performed in this work are via the commercially available (high frequency structure simulator) HFSS software.

3. Results and Discussion

Figure 3 shows the simulated and measured return losses of the proposed tag antenna in planar form (free-space condition, FSC). The simulated and measured return losses when attaching this tag antenna to a human wrist are also plotted in this figure. When comparing the impedance bandwidths, the simulated 6-dB return loss bandwidth in FSC was 5.2% (0.89–0.938 GHz), while the measured one was 3.9% (0.9–0.936 GHz). The slight differences between the two results may be due to fabrication tolerance and unexpected effects, especially when the slotted patch was soldered to the two copper tapes located on the top surface of the PVC. Nonetheless, the measured resonant mode of the proposed one in FSC was 914 MHz, while the measured one on human wrist was slightly lower at 904 MHz. Notably, the simulated 6-dB return loss bandwidth of proposed tag antenna attached to human wrist was 6.2% (0.88–0.937 GHz), and its corresponding measured one was 5.3% (0.88–0.928 GHz). Here, the differences between the two results can be attributed to the under estimated parameters (dielectric constant, loss tangent, and conductivity) given in [4, 5]. Furthermore, as shown in Figure 4, the measurement that we have conducted was by applying the 1/4 wavelength balun technique studied in [13], which may yield slight inaccuracy during actual measurement.

To validate the above results, Figures 5(a) and 5(b) show the input resistance and reactance of the proposed tag antenna, respectively, corresponding to the ones shown in Figure 3. As depicted in Figure 5(a), even though the results for the measured input resistance in FSC and human wrist are higher (approximately 9.3 Ω and 13 Ω, respectively) than the tag chip resistance (8 Ω), their respective reactance as shown

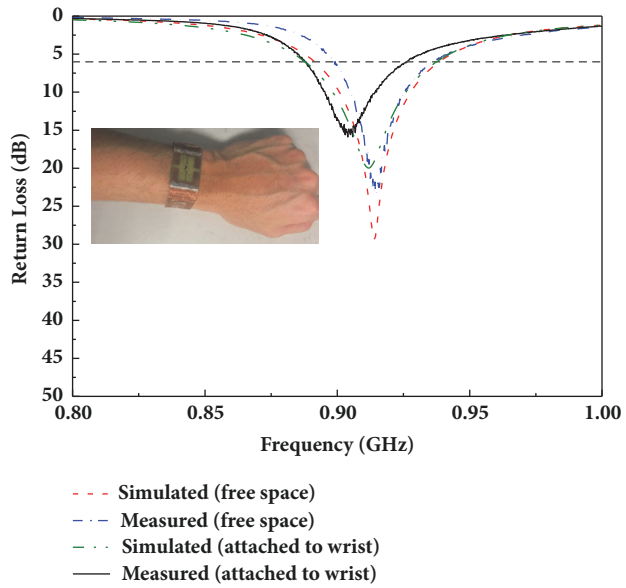

Figure 3: Simulated and measured return losses of the proposed tag antenna at free-space (planar form) and attached to wrist conditions.

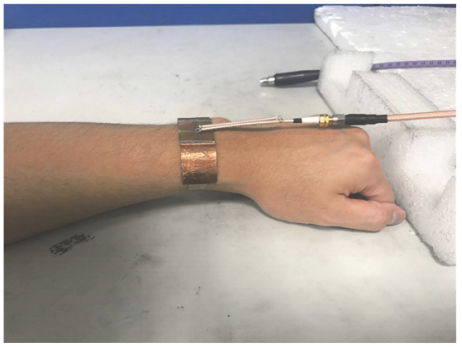

Figure 4: Measurement of the proposed tag antenna on human wrist by applying the 1/4 wavelength balun technique [13].

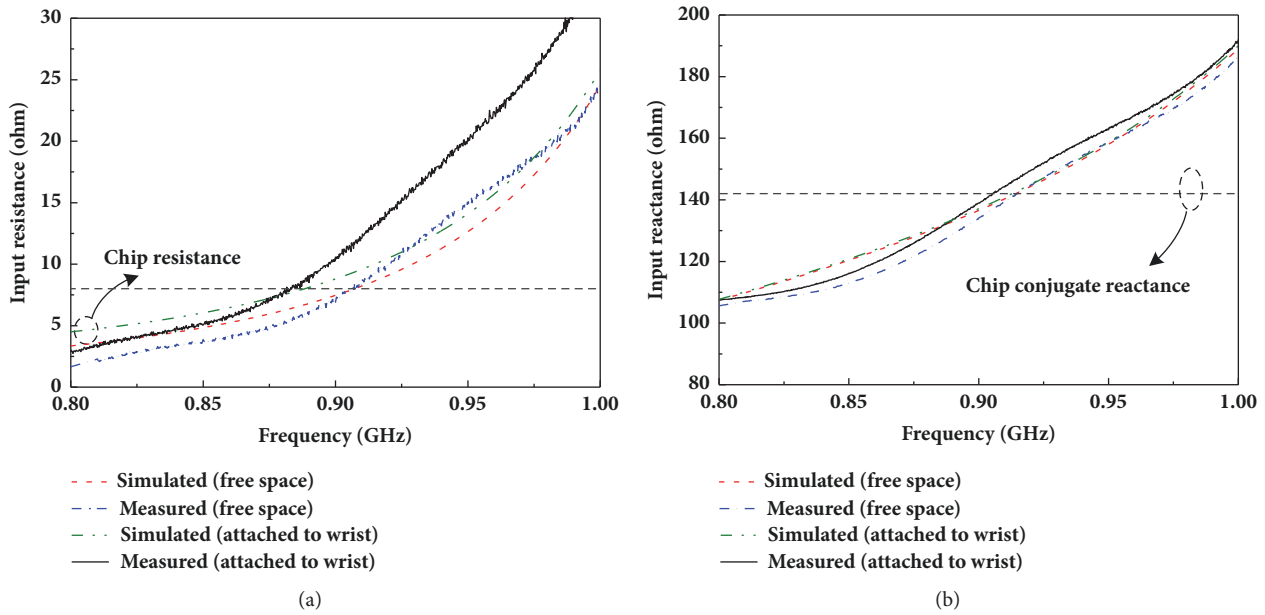

Figure 5: Simulated and measured input impedance of the proposed tag antenna in FSC and when attached to human wrist: (a) resistance and (b) reactance.

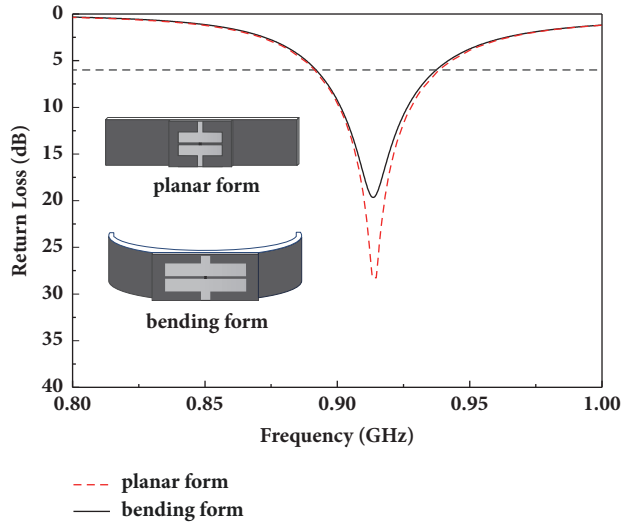

FIGURE 6: Simulated return losses of the proposed tag antenna in FSC and in planar form and bending form.

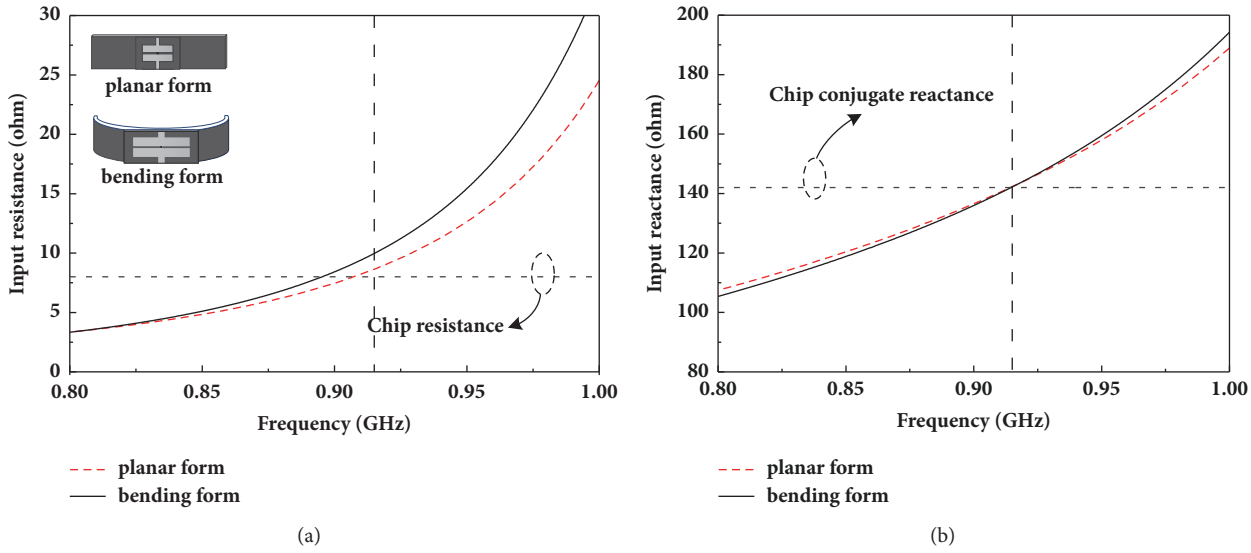

FIGURE 7: Simulated input resistance and reactance of proposed tag antenna in FSC in planar form and bending form.

in Figure 5(b) is very much well conjugate with the tag chip reactance ($-j142\ \Omega$) at around 915 MHz.

3.1. Effects of Bending the Tag Antenna. Figure 6 shows the simulated return losses of proposed antenna in FSC, when the antenna is simply a planar type (no bending) and when it is bent to conform to a normal human wrist. As depicted in this figure, bending the proposed tag antenna will only slightly affect the impedance matching, which can be clearly explained in Figure 7(a), showing a slightly deviated input resistance value at around 915 MHz, whereas its corresponding reactance remains unchanged, as shown in Figure 7(b).

3.2. Effects of Tuning the Parameter d. To allow this proposed tag antenna to be able to work across the desired UHF RFID frequency band (902–928 MHz), it is important to identify the one parameter of the tag antenna structure that can easily aid in tuning the excited resonant frequency. As depicted in Figure 8, it is realized that increasing parameter d from 24 mm to 28 mm (with a step increment of 2 mm), meaning also that the total length of tag antenna will also be increased from 82 mm to 90 mm, can allow linear shifting of the resonant frequency to the lower frequency from 950 MHz to 880 MHz. To further understand this phenomenon, the simulated input resistance and input reactance of the proposed tag antenna when tuning parameter d are also presented in Figures 9(a) and 9(b), respectively. By further observing these two figures, it is also realized that increasing d will linearly decrease both the input resistance and reactance of the proposed tag antenna, respectively, which explains the shift to the lower frequency band.

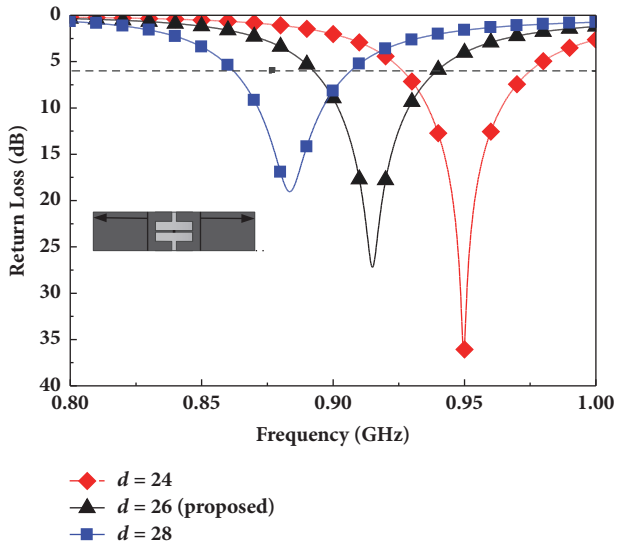

Figure 8: Simulated return losses of the proposed tag antenna when tuning parameter d. Unit: mm.

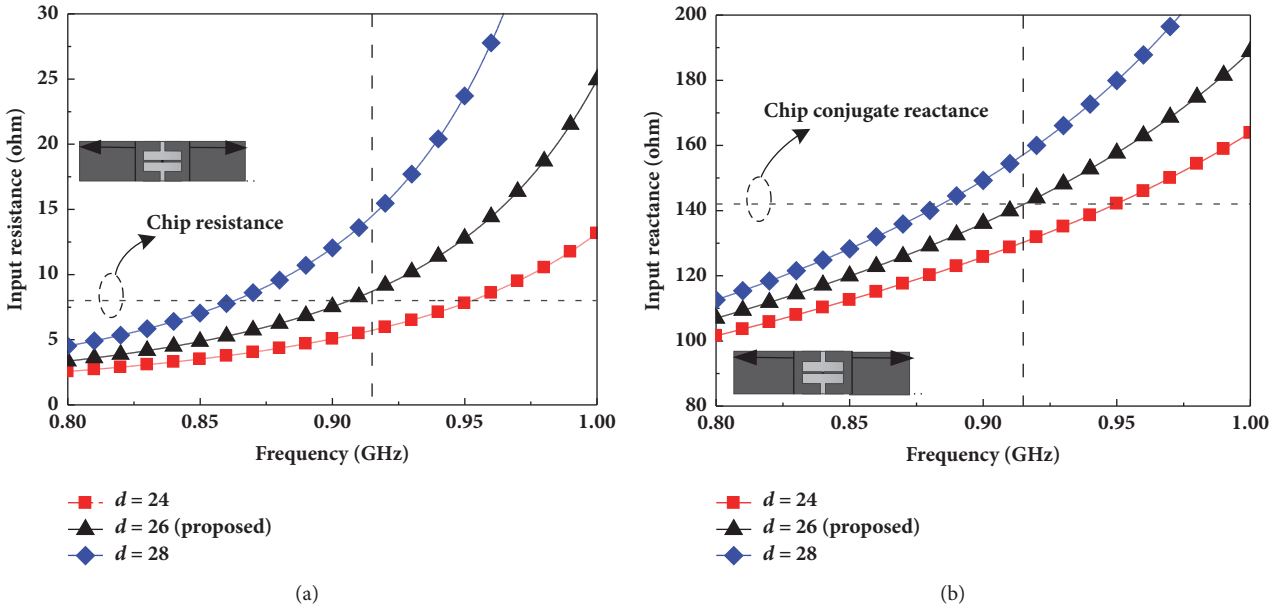

Figure 9: Simulated impedance of proposed tag antenna when tuning parameter d, (a) input resistance and (b) input reactance. Unit: mm.

As for the reason why increasing the parameter d can decrease the resistance and reactance, one can see from Figure 1 that the proposed tag antenna is a folded type, thus, increasing parameter d which will also increase the folded surface area (top and bottom), resulting in an increase in capacitive reactance. Thus, once the capacitive reactance (X_c) is increased, the inductive reactance (X_L) of this proposed tag antenna will be decreased. As the inductive reactance $X_L = 2\pi f$ L, a decrease in X_L will obviously result in a decreased frequency. Notably, reducing the overall reactance of the proposed tag antenna by increasing parameter d may be the main reason why the resistive value is also decreased. Another explanation can also be related to the electrical wavelength, which indicates that the longer the electrical length (including the length d), the longer the wavelength, thus achieving lower frequency.

Therefore, this proposed tag antenna has possessed the advantage of ease in tuning the resonance frequency.

3.3. Effects of Tuning Parameter S_l. As aforementioned, the slotted patch is responsible for tuning the impedance matching of the proposed tag antenna. As the slotted patch is composed of two symmetrical T-shaped slots, tuning any of its slot's parameters (S_l, S_w, and S_g) requires both T-shaped slots to be tuned at the same time; however, the width of narrow feeding line must remain constant at 1 mm for ease in attaching the tag chip that has the same width of 1 mm. The simulated effects of tuning the parameter S_l are first

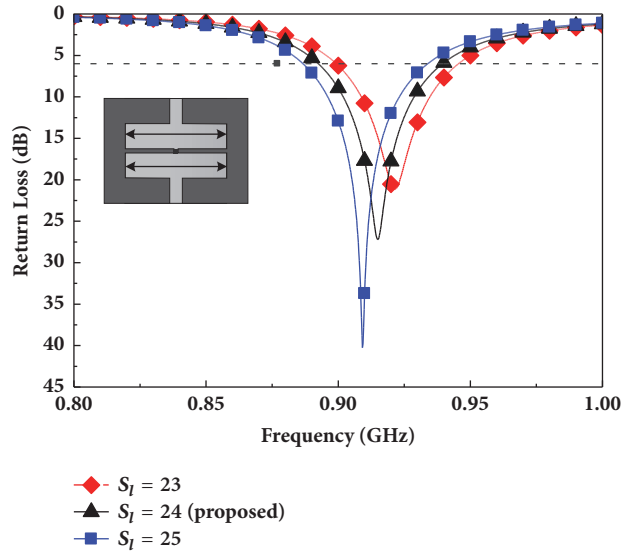

FIGURE 10: Simulated return losses of the proposed tag antenna when tuning parameter S_l. Unit: mm.

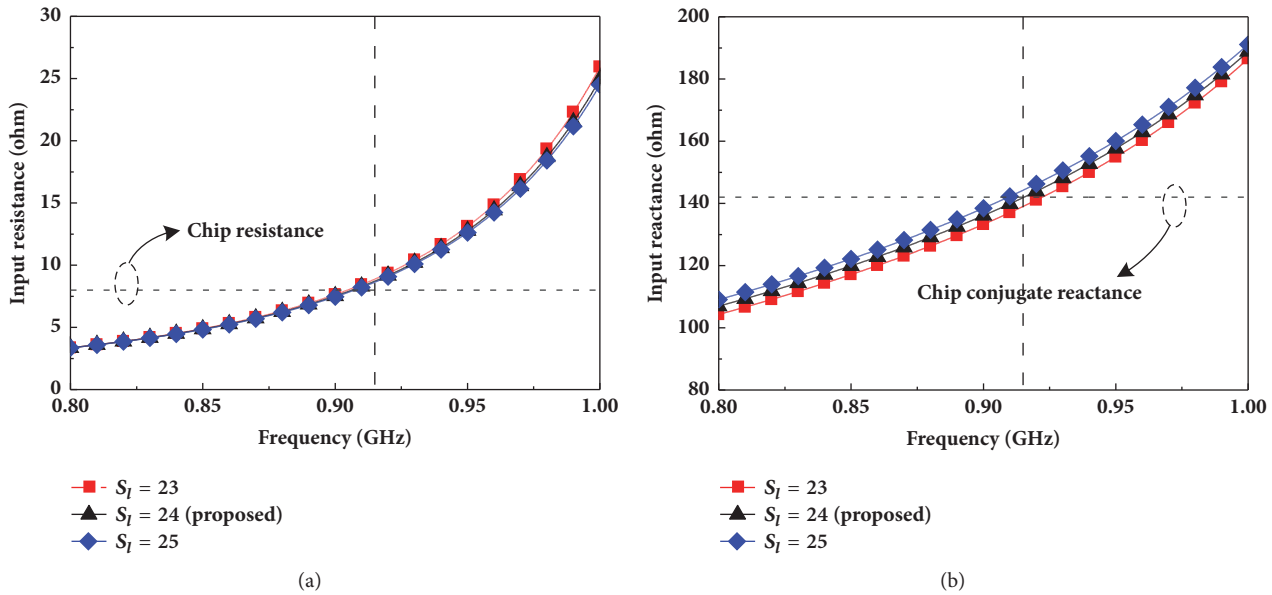

FIGURE 11: Simulated impedance of proposed tag antenna when tuning parameter S_l, (a) input resistance and (b) input reactance. Unit: mm.

investigated and shown in Figures 10 and 11, while the other two parameters (S_w, and S_g) remain constant.

As depicted in Figure 10, it is realized that increasing parameter S_l from 23 mm to 25 mm (with a step increment of 1 mm) can allow linear shifting of the resonant frequency to the lower frequency from 921 MHz to 909 MHz. Its corresponding simulated input resistance and input reactance are also plotted in Figures 11(a) and 11(b), respectively. By further observing these two figures, it is realized that tuning S_l will not affect the input resistance values at 915 MHz, but rather the input reactance at 915 MHz has slightly raised as S_l increases. In addition to that, the entire input reactance has shifted to the lower frequency, which validated with the trend observed in Figure 10.

3.4. Effects of Tuning Parameter S_w. Figure 12 shows the effects on the return losses of the proposed tag antenna when increasing the slot's parameter S_w from 5 mm to 7 mm (with a step increment of 1 mm). Here, increasing S_w will allow slight linear shifting of the resonant frequency to the upper frequency from 906 MHz to 923 MHz. To further understand this phenomenon, the simulated input resistance and input reactance of the proposed tag antenna when tuning parameter S_w are also presented in Figures 13(a) and 13(b),

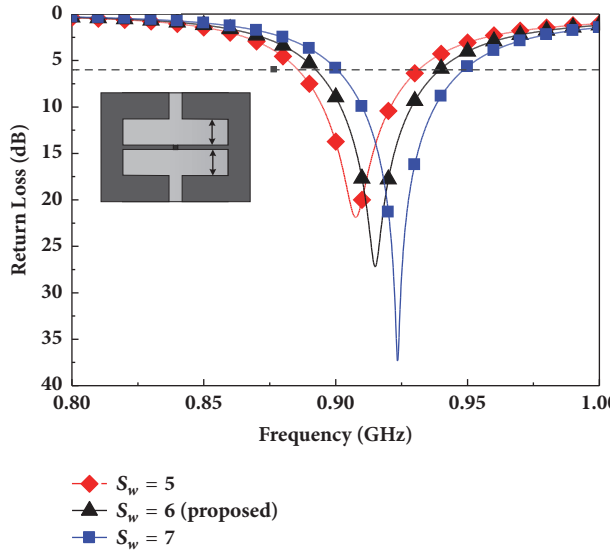

FIGURE 12: Simulated return losses of the proposed tag antenna when tuning parameter S_w. Unit: mm.

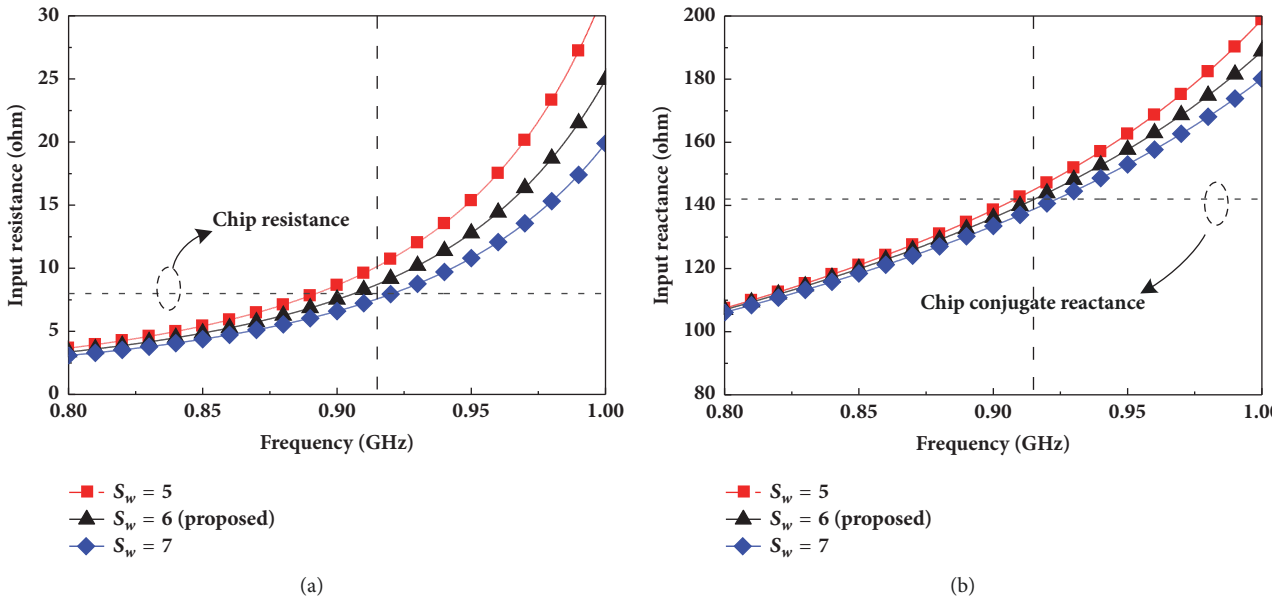

FIGURE 13: Simulated impedance of proposed tag antenna when tuning parameter S_w. (a) Input resistance and (b) input reactance. Unit: mm.

respectively. By further observing these two figures, it is also realized that increasing S_w will linearly shift the entire input resistance and reactance of the proposed tag antenna to the higher frequency band.

3.5. Effects of Tuning Parameter S_g. The effects on the return losses of the proposed tag antenna when increasing the slot's parameter S_g from 2 mm to 4 mm (with a step increment of 1 mm) are shown in Figure 14. In this figure, it is realized that increasing parameter S_g can allow linear shifting of the resonant frequency to the higher frequency from 910 MHz to 920 MHz. From its corresponding simulated input resistance and input reactance plotted in Figures 15(a) and 15(b), respectively, it is also realized that increasing S_g will also linearly shift the entire input resistance and reactance of the proposed tag antenna to the higher frequency band.

Therefore, from the above parametric results, the following conclusions can be drawn: (1) tuning d can easily achieve good resonant frequency and operating bands across the entire UHF RFID band in EPC Gen 2 (Electronic Product Code Generation 2, 860–960 MHz), (2) tuning S_l will only affect the input reactance while the input resistance remains constant, and (3) tuning both S_w and S_g will affect input reactance and resistance values.

3.6. Simulated Radiation Patterns. The simulated radiation patterns at 915 MHz (in three different principle planes) of

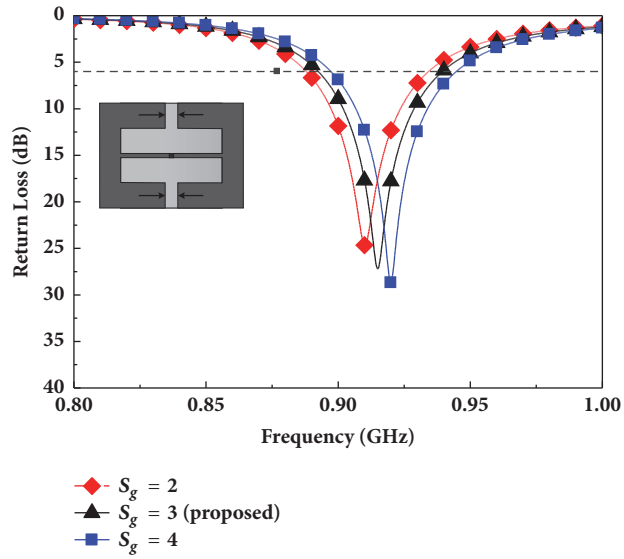

FIGURE 14: Simulated return losses of the proposed tag antenna when tuning parameter S_g. Unit: mm.

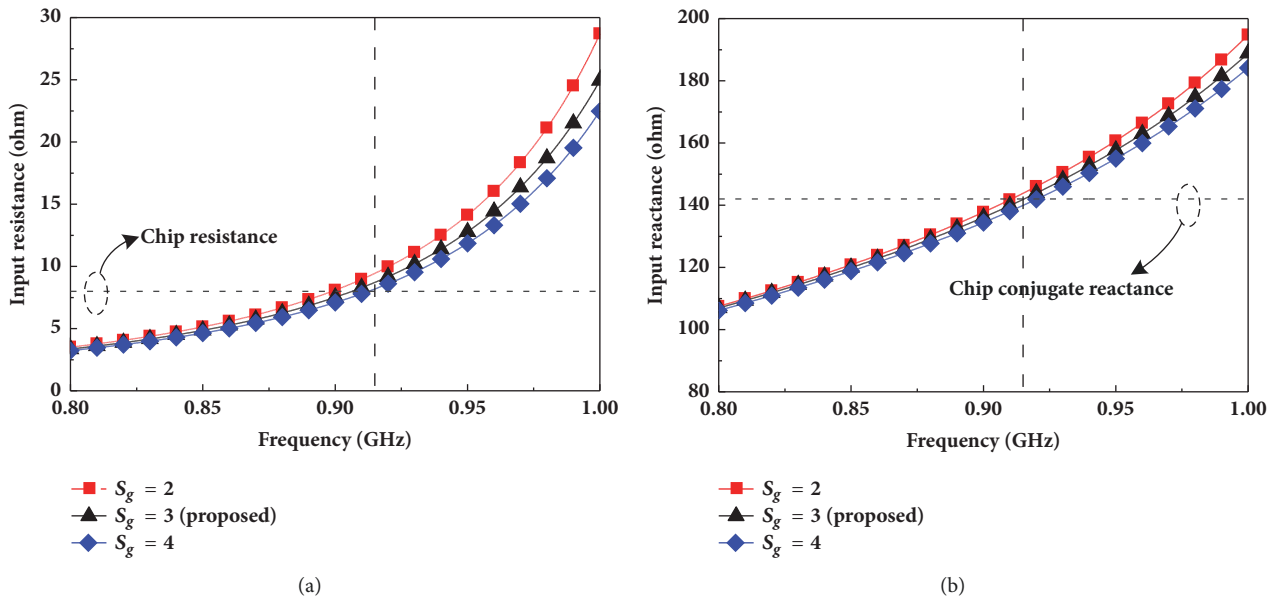

FIGURE 15: Simulated impedance of proposed tag antenna when tuning parameter S_g, (a) input resistance and (b) input reactance. Unit: mm.

the proposed tag antenna in planar form and attached to a human wrist phantom (indicated in Figure 2 and Table 1) are shown in Figures 16 and 17, respectively, and all values are normalized with respect to their peak gain. As shown in Figure 16, good omnidirectional patterns for E_ϕ were observed in the x-z plane, while good broadside patterns in the $\pm z$ directions were observed for E_θ in the y-z plane. Obvious bidirectional patterns were also observed in its corresponding x-y plane. As depicted in Figure 17, both the x-z and y-z planes have shown an obvious decrease in signal strength (approximately 5 to 6 dB) in the $-z$ direction (θ = 180°) as compared with its corresponding boresight direction ($+z$, θ = 0°). By comparing these two figures, it can be denoted that the human wrist can absorb the signal strength (EM wave) that is propagating towards the wrist (in the $-z$ direction). Furthermore, the boresight signal strength (or peak gain at $+z$ direction) has also been reduced from -4.62 dBi to -6.87 dBi, due to the effects of the human wrist.

3.7. Measured Maximum Reading Range of Proposed Tag Antenna. To perform the maximum reading range (R_{max}) of this proposed tag antenna in a more accurate manner, two experiments were setup via a commercially available equipment known as "Voyantic Tagformance Pro", which is

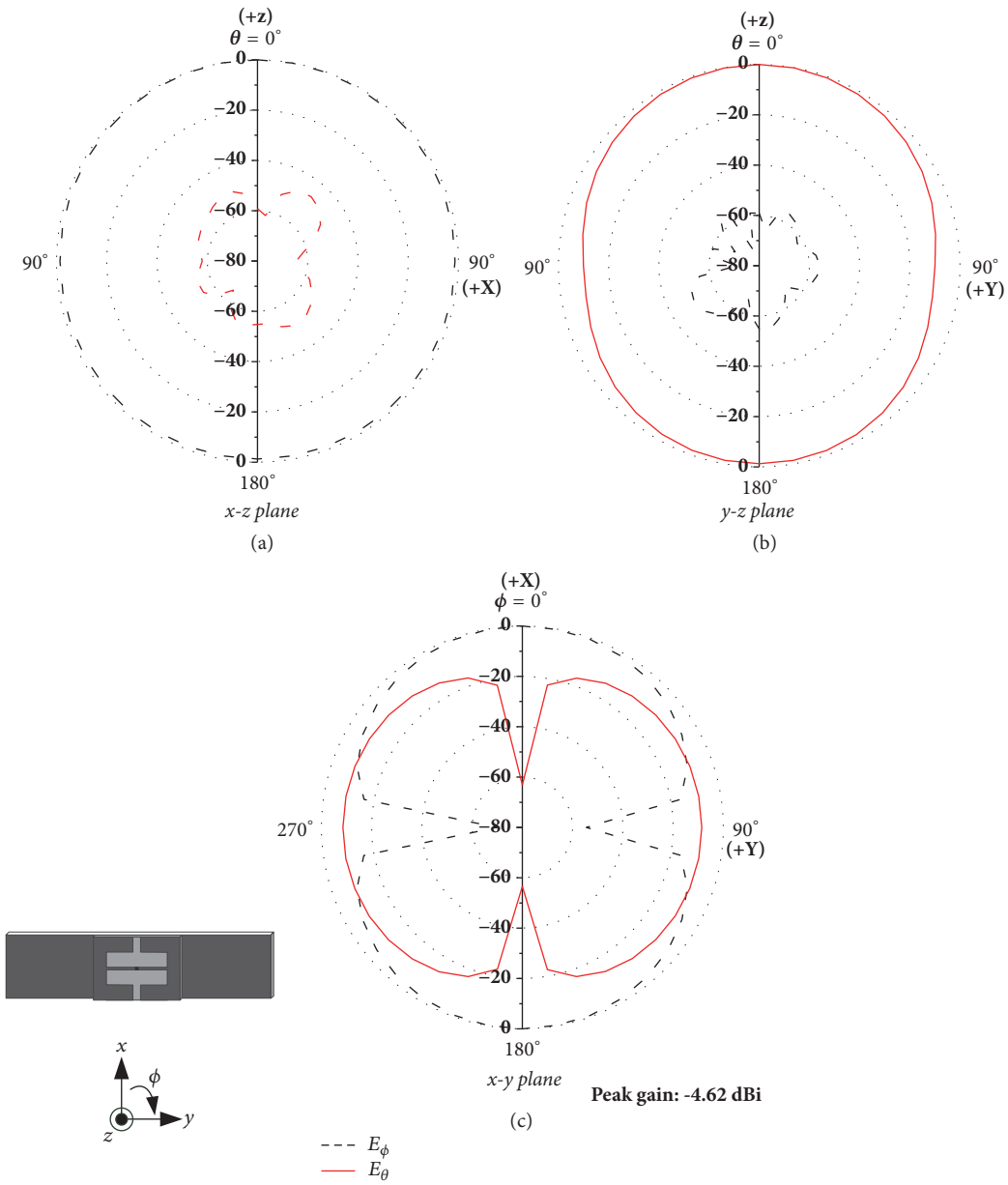

FIGURE 16: Simulated radiation patterns (normalized) of the proposed tag antenna (planar form) at 915 MHz.

an all-in-one test and measurement device for UHF RFID tag antenna [14]. The first setup of the measurement is as shown in Figure 18, in which the proposed tag antenna was attached to a piece of fresh pork. Even though the thicknesses of skin, fat, and muscle of this fresh pork are not the same as human wrist, the reason for using pork is because its electrical properties (fat and muscle) are very much closer to the human ones. Furthermore, it is very easy to obtain, rather than the commercialized hand phantom that is very expensive and not available to the authors. The illustration of this equipment setup is shown in Figure 19, in which a standard horizontal linearly polarized transmitting antenna (7.2 dBi gain) was used in this case and connected to an RF output power of no more than 0.5 W (27 dBm). Thus, the total EIRP (effective isotropic radiation power) applied in this case for the measurement was 2.63 W (34.2 dBm). As for the second setup, the AUT (antenna under test) was simply replaced with a planar type proposed tag antenna without the attached pork.

Figures 20 and 21 show the measurement results obtained by the two experimental setups performed in the "Voyantic Tagformance Pro" chamber. As depicted in Figure 20, R_{max} of the proposed tag antenna in planar form (FSC) measured across 900–930 MHz were approximately between 6.6 m and 8.0 m. As for the case when it was attached to a piece of pork, its corresponding R_{max} were measured approximately

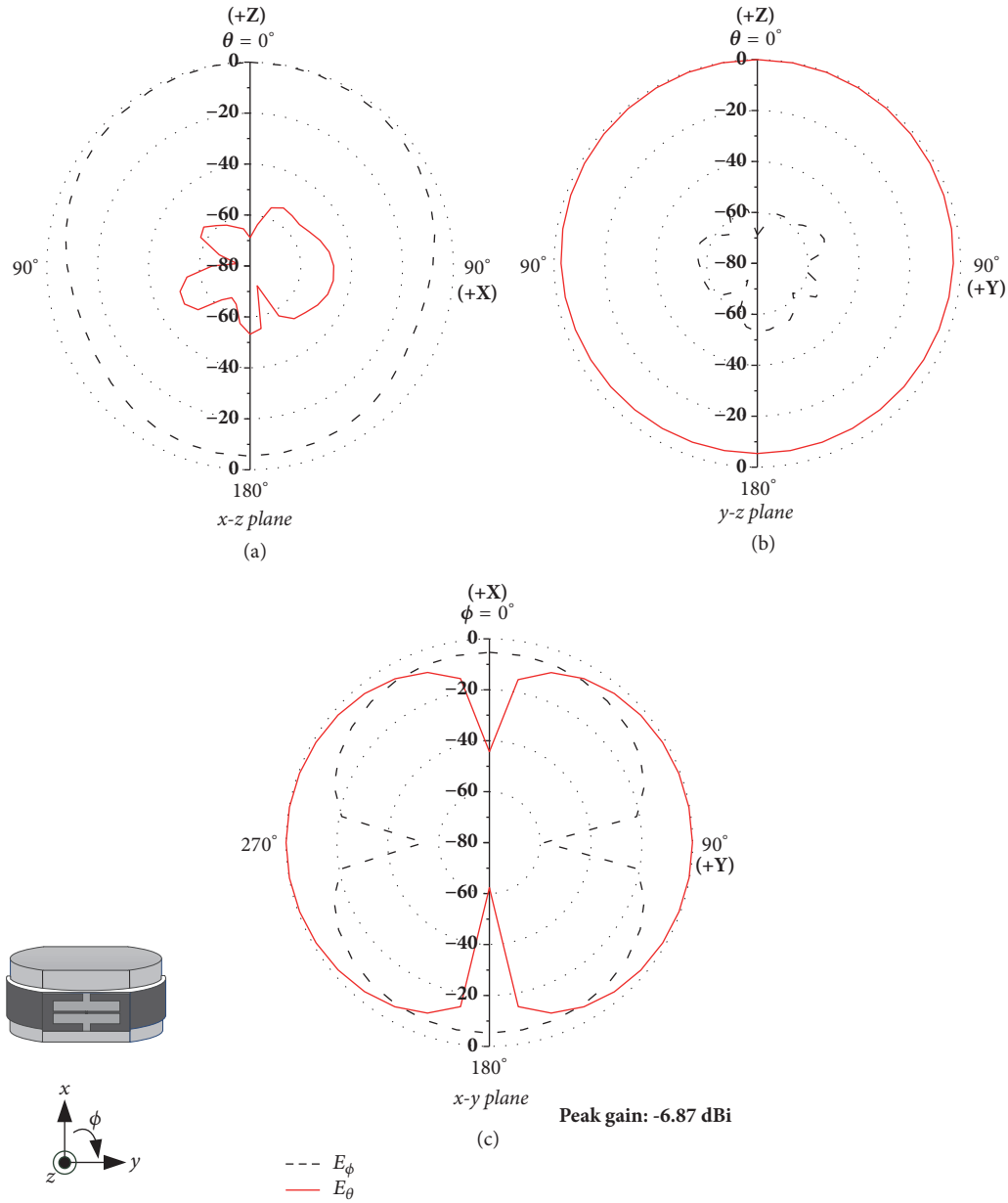

FIGURE 17: Simulated radiation patterns (normalized) of proposed antenna (attached to a human wrist phantom) at 915 MHz.

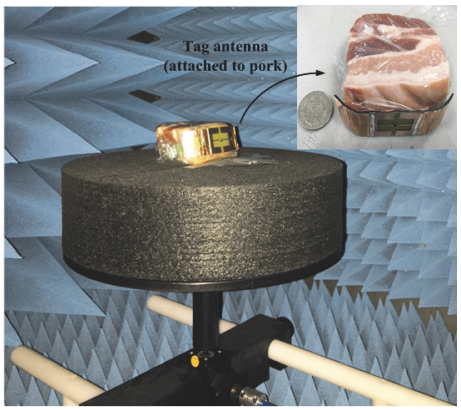

FIGURE 18: Photograph of proposed tag antenna attached to a piece of pork and placed in a "Voyantic Tagformance Pro" chamber [14] ready for measurement.

between 6 m and 6.6 m (across 900–930 MHz). Figure 21 shows the measured R_{max} of the proposed tag antenna at 915 MHz across the azimuth plane (y-z plane) for the two setup cases. Here, in planar form (FSC), the boresight direction ($+z$ direction) has shown R_{max} of 8 m, and it will slowly mitigate when the θ angle has shifted away from boresight direction. In addition to that, R_{max} will reach a minimum range of approximately 2.2 m when the θ angle is at 90° or 270°. As discussed earlier, because of the absorption from the pork, the proposed tag antenna attached to pork has a lower R_{max} of 6.6 m as compared with the planar form case at boresight direction. Furthermore, this absorption by the pork will become more prominent for the $-z$ direction, showing a reduced R_{max} of 4.08 m, as compared with the planar form case with R_{max} = 7.18 m. From the above results, because the proposed tag antenna (for the two setup cases) has shown

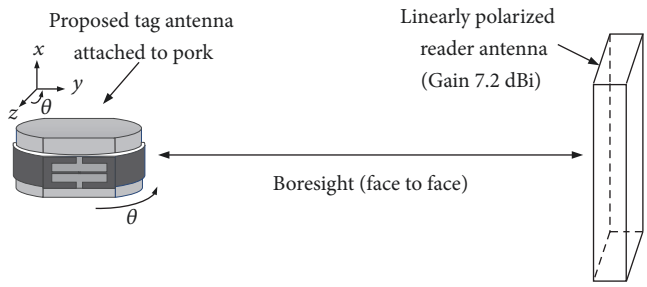

FIGURE 19: The illustration of proposed tag antenna attached to a piece of pork and placed in a "Voyantic Tagformance Pro" chamber that has a linearly polarized reader antenna with EIRP = 2.63 W.

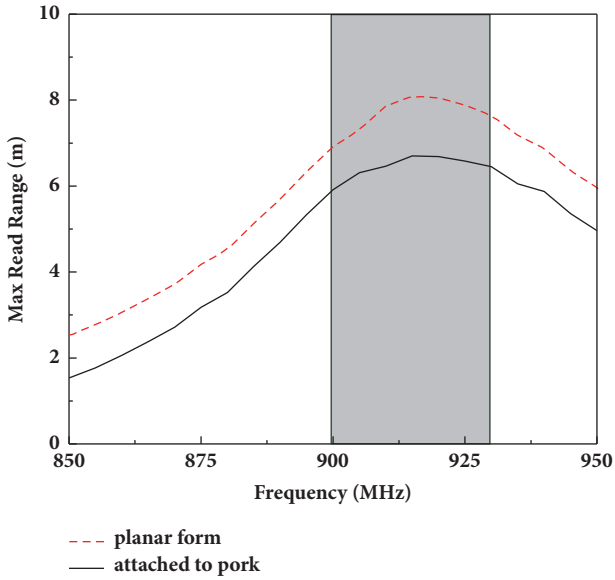

FIGURE 20: Maximum reading range measurement of the proposed tag antenna (with and without attached to a piece of pork) performed by a "Voyantic Tagformance Pro" chamber [14].

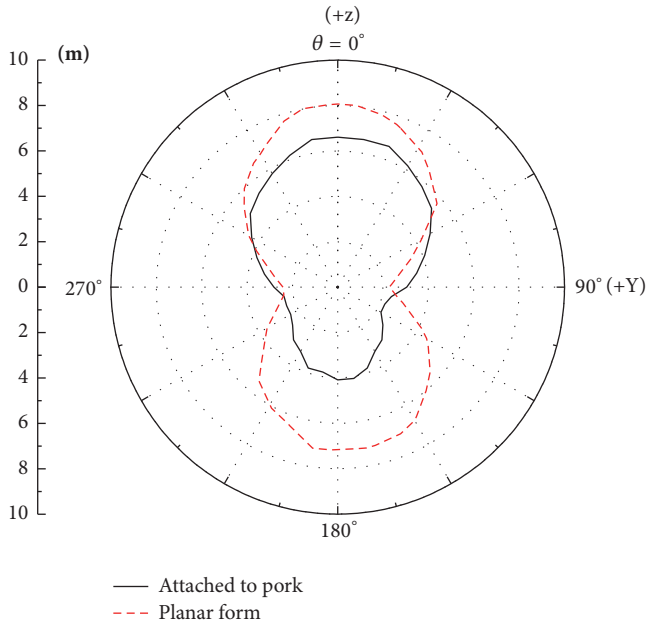

FIGURE 21: Measured reading ranges of the proposed tag antenna for the two setup cases at 915 MHz across the azimuth plane (*y*-*z* plane) performed by the "Voyantic Tagformance Pro" chamber.

minimum R_{max} of at least 2 m (EIRP 2.63 W) across the entire azimuth, it is therefore suitable for incorporating into the healthcare applications for tracking/monitoring the patients.

To further validate the above results, the proposed antenna was placed into the wrist of three volunteers standing in a non-free-space condition (non-FSC) environment. As shown in Figure 22, the volunteers were standing in the middle of two rows of metal tables in the laboratory, creating a narrow and crowded environment with multipath condition. From the measurement via an RFID reader system (Favite) with 2.63W (34.2 dBm) EIRP, the measured distances performed on these three different students were 3.1 m, 3 m, and 3.2 m, which are approximately half the distance measured in FSC using the "Voyantic Tagformance Pro" chamber. However, one needs to take note that these measurements were taken in a very undesirable condition (narrow and crowded environment with metal walls on both sides), and thus the results obtained may vary across different environments.

4. Conclusions

A simple low-profile flexible RFID tag antenna has been successfully studied for working in the UHF band (902–928 MHz). The proposed open-slot cavity design of this tag antenna has the advantages of ease in impedance matching and tuning to the desired frequency band. The 6-dB return loss bandwidth of the proposed tag antenna when attached to a human wrist was 5.3% (0.88–0.928 GHz). In free-space condition, the experimental result shows that the proposed tag antenna can exhibit good reading ranges of between 2.2 m and 6.6 m. In a narrow and crowded environment with metal walls on both sides, at boresight direction, the reading range can be up to 3 meters. Therefore, this proposed antenna is a good candidate for tracking/monitoring the patients for future healthcare industry.

Figure 22: Measured reading ranges of proposed tag antenna on the wrist of three volunteers in a very narrow and crowded environment with metal tables on both sides.

Conflicts of Interest

The authors declare that they have no conflicts of interest.

References

[1] M. A. Ziai and J. C. Batchelor, "A prototype passive UHF RFID transfer tattoo tag," in *Proceedings of the 5th European Conference on Antennas and Propagation, EUCAP 2011*, pp. 3811–3814, April 2011.

[2] T. Kellomäki, "On-body performance of a wearable single-layer RFID tag," *IEEE Antennas and Wireless Propagation Letters*, vol. 11, pp. 73–76, 2012.

[3] S. Amendola, S. Milici, and G. Marrocco, "Performance of epidermal RFID dual-loop tag and on-skin retuning," *IEEE Transactions on Antennas and Propagation*, vol. 63, no. 8, pp. 3672–3680, 2015.

[4] Y. Jin, J. Tak, and J. Choi, "Compact dual-band antenna for smart wristband application," *Microwave and Optical Technology Letters*, vol. 58, no. 6, pp. 1462–1466, June, 2016.

[5] http://niremf.ifac.cnr.it/tissprop/.

[6] S. Amendola, G. Bovesecchi, A. Palombi, P. Coppa, and G. Marrocco, "Design, Calibration and Experimentation of an Epidermal RFID Sensor for Remote Temperature Monitoring," *IEEE Sensors Journal*, vol. 16, no. 19, pp. 7250–7257, 2016.

[7] G. Marrocco, "RFID antennas for the UHF remote monitoring of human subjects," *IEEE Transactions on Antennas and Propagation*, vol. 55, no. 6, pp. 1862–1870, 2007.

[8] A. Dubok and A. B. Smolders, "Miniaturization of robust UHF RFID antennas for use on perishable goods and human bodies," *IEEE Antennas and Wireless Propagation Letters*, vol. 13, pp. 1321–1324, 2014.

[9] M. C. Tsai, I. G. Li, C. W. Chiu, and H. C. Wang, "UHF RFID PIFA array tag antenna for human body applications," in *Proceedings of the 15th Int. Symposium on WPMC*, pp. 434–437, September, 2012.

[10] M. Svanda and M. Polivka, "On-body semi-electrically-small tag antenna for ultra high frequency radio-frequency identification platform-tolerant applications," *IET Microwaves, Antennas & Propagation*, vol. 10, no. 6, pp. 631–637, 2016.

[11] H. Rajagopalan and Y. Rahmat-Samii, "On-body RFID tag design for human monitoring applications," in *Proceedings of the IEEE Antennas Propagation Soc. Int. Symp.*, pp. 1–4, July, 2010.

[12] S. Lopez-Soriano and J. Parron, "Low profile UHF RFID tag for wristbands in healthcare applications," in *Proceedings of the 8th European Conference on Antennas and Propagation, EuCAP 2014*, pp. 874–877, April 2014.

[13] H.-G. Cho, N. R. Labadie, and S. K. Sharma, "Design of an embedded-feed type microstrip patch antenna for UHF radio frequency identification tag on metallic objects," *IET Microwaves, Antennas & Propagation*, vol. 4, no. 9, pp. 1232–1239, 2010.

[14] "Tagformance-pro," http://voyantic.com/products/tagformance-pro.